



Use of pyrophyllite clay for fluoride removal from aqueous solution

Jae-Hyun Kim^a, Chang-Gu Lee^a, Jeong-Ann Park^a, Jin-Kyu Kang^a, Nag-Choul Choi^b, Song-Bae Kim^{b,*}

^a*Environmental Functional Materials & Biocolloids Laboratory, Seoul National University, Seoul 151-921, Korea*

^b*Department of Rural Systems Engineering/Research Institute for Agriculture and Life Sciences, Seoul National University, Seoul 151-921, Republic of Korea*

Tel. +82 2 880 4587; Fax: +82 2 873 2087; email: songbkim@snu.ac.kr

Received 10 February 2012; Accepted 10 October 2012

ABSTRACT

The aim of this study was to investigate the removal of fluoride from aqueous solution using pyrophyllite clay as an adsorbent. X-ray fluorescence analysis showed that Si (74.03%) and Al (21.20%) were the major constituents of pyrophyllite. Equilibrium test (adsorbent particle size <0.15 mm) demonstrated that the maximum sorption capacity of pyrophyllite was 0.737 mg/g. Kinetic test showed that fluoride sorption to pyrophyllite arrived at equilibrium around 24 h. Thermodynamic test indicated that fluoride sorption to pyrophyllite increased with increasing temperature from 25 to 45 °C, indicating the endothermic nature of sorption process. Further experiments indicated that fluoride removal was not sensitive to solution pH between 4.0 and 9.0. The influence of sulfate, carbonate, and phosphate on the removal of fluoride was important while the effect of nitrate and chloride was negligible. In addition, among the pyrophyllite thermally treated at different temperatures (untreated, 400, 600, 800, 1,000, 1,000 °C), the adsorbent treated at 400 °C had the highest adsorption capacity (21% higher than that of untreated pyrophyllite). This study demonstrates the potential use of pyrophyllite for fluoride removal from water.

Keywords: Adsorbent; Batch experiment; Defluoridation; Sorption; Thermal treatment

1. Introduction

Fluoride contamination of drinking water resources is a serious environmental problem around the world. In many countries such as India, China, the Middle East, and African countries, fluoride occurs naturally in groundwater at concentrations exceeding the guidelines of the World Health Organization (1.5 mg/L), causing serious health problems. At the concentration of >1.5 mg/L, fluoride could cause neurological damages and dental/skeletal fluorosis [1].

For the removal of fluoride from water, adsorption is widely used mainly because of cost-effectiveness and simplicity of operation. Various adsorbents have been used for fluoride removal, including activated alumina, activated carbon, granular ferric hydroxide, limestone, fly ash, etc. [2]. The use of clays to remove fluoride has also been investigated by several researchers [2,3]. They have examined the adsorption of fluoride to china clay [4], fluoride removal by montmorillonite under various contact times and temperatures [5], treatment of high fluoride solution by Mg/Al layered double hydroxide [6], and fluoride

*Corresponding author.

adsorption to montmorillonite with and without calcium [7]. They also investigated the removal of fluoride by acid activated kaolinite [8], adsorption of fluoride to metal oxide incorporated bentonite [9], and enhancement of fluoride removal by chemically modified bentonite with magnesium chloride [10].

Pyrophyllite is a 2:1 clay mineral with dioctahedral structure consisting of neutral tetrahedral–octahedral–tetrahedral layers. It is a hydrous aluminosilicate clay with the chemical composition of $\text{AlSi}_2\text{O}_5(\text{OH})$. Pyrophyllite has many industrial applications, especially as a raw material in the ceramic, glass, and refractory industries [11]. Recently, pyrophyllite has been examined as an adsorbent for the removal of contaminants such as boron, cyanide, heavy metals, and dyes [12–16]. In addition, pyrophyllite has been used for fluoride removal from aqueous solution [17]. Further experiments will improve our knowledge regarding the potential uptake of fluoride by pyrophyllite.

The objective of this study was to investigate the removal of fluoride from aqueous solution using pyrophyllite clay as an adsorbent. The characteristics of pyrophyllite were elucidated using X-ray fluorescence (XRF) spectrometer, X-ray diffraction (XRD) spectrometer, field emission scanning electron microscopy (FESEM) and Fourier transform infrared (FTIR) spectrometer. Equilibrium, kinetic, and thermodynamic experiments were performed to examine the adsorption of fluoride to pyrophyllite. The effects of adsorbent dose, pH, and competing anions on the adsorption of fluoride were also observed. Finally, thermal treatment of pyrophyllite on the adsorption of fluoride was examined.

2. Materials and methods

2.1. Preparation and characterization of pyrophyllite

Pyrophyllite used in this study was obtained from the Sungsan mining in Haenam, Korea. Mechanical sieving was conducted with US Standard Sieves No. 100. Pyrophyllite fractions with a grain size of less than 0.15 mm were used unless stated otherwise. FESEM and Energy Dispersive X-ray Spectrometer (EDS) analyses were performed using a FESEM (Supra 55VP, Carl Zeiss, Germany). The chemical composition of pyrophyllite was investigated using an (XRF, S4 pioneer, Bruker, Germany). Surface area was determined by Brunauer–Emmett–Teller (BET) N_2 adsorption analysis using an ASAP 2010 instrument (Micromeritics, USA). The mineralogical and crystalline structural properties were examined using (XRD, D8 Advance, Bruker, Germany) with a $\text{CuK}\alpha$ radiation of 1.5406 Å at a scanning speed of $0.6^\circ/\text{sec}$. Infrared spectra were

recorded on a Bomem MB-104 (Abb-Bomem Inc., Quebec, Canada) FTIR spectrometer using KBr pellets. The zeta potentials were measured at various pH values, which were obtained using dilute HNO_3 and NH_4OH . The point of zero charge (pH_{pzc}) of pyrophyllite was determined from the zeta potentials.

2.2. Batch experiments

All chemicals used for the experiments were purchased from Sigma Aldrich. The desired fluoride solution was prepared by diluting the stocking fluoride solution (1,000 mg/L), which was made from sodium fluoride (NaF). All batch experiments were performed at a solution pH of 5.5 unless stated otherwise. Equilibrium batch experiments were conducted with four different particle sizes of pyrophyllite. One gram of pyrophyllite was added to 30 mL fluoride solution (initial concentration = 4–96 mg/L) in 50 mL polypropylene conical tubes. The tubes were shaken at 25°C and 40 rpm using a culture tube rotator (MG-150D, Mega Science, Korea). The samples were collected 24 h post-reaction, and filtered through a $0.45\ \mu\text{m}$ membrane filter. The fluoride concentration was measured using fluoride ion selective electrode (9609BNWP, Thermo Scientific, USA). In the fluoride measurement, total ionic strength adjustment buffer solution (58 g NaCl, 57 mL CH_3COOH , 150 mL 6 M NaOH in 1,000 mL deionized water) was used to prevent the interference of other ions.

Next, kinetic batch experiments were performed at the initial fluoride concentration of 10 mg/L and pyrophyllite dose of 1 g. In the experiments, the samples were taken at 1, 2, 3, 6, 9, 12, 24, 36 and 48 h post-reaction. Thermodynamic experiments were conducted at 25, 35, and 45°C to observe the effect of temperature on fluoride removal. The experiments were performed at the initial fluoride concentration of 10 mg/L and pyrophyllite dose of 1 g, and the samples were taken at 1, 2, 3, 6, 9, 12, 24, 36 and 48 h post-reaction. Further batch experiments were carried out to examine the effect of pyrophyllite dosage on fluoride removal. The experiments were conducted at an initial fluoride concentration of 10 mg/L with pyrophyllite dosages ranging from 0.05 to 2.0 g in 30 mL solution. The samples were collected 24 h post-reaction.

In the pH experiments, 0.1 M NaOH and 0.1 M HCl solutions were used for adjusting the pH from 2.9 to 11.0. The pH was measured with a pH probe (9107BN, Thermo Scientific, USA). In the competing anion experiments, the competing anions (Cl^- , NO_3^- , SO_4^{2-} , HPO_4^{2-} , CO_3^{2-}) were added to fluoride solution to achieve the desired anion concentrations (0.5, 1 mM). Lastly, batch experiments were performed to

examine the effect of thermal treatment of pyrophyllite on fluoride removal (initial fluoride concentration = 10 mg/L; pyrophyllite dose = 0.6 g). Pyrophyllite was thermally treated at different temperature for 3 h in a programmable tube furnace (WiseTherm(R) FT-1230, DAIHAN Scientific, Korea). All experiments were performed in triplicate.

2.3. Data analysis

The equilibrium data can be analyzed using the following Langmuir and Freundlich isotherm models:

$$q_e = \frac{Q_m K_L C_e}{1 + K_L C_e} \quad (1)$$

$$q_e = K_F C_e^n \quad (2)$$

where q_e is the amount of fluoride removed at equilibrium (mg/g), Q_m is the maximum mass of fluoride removed per unit mass of pyrophyllite (removal capacity) (mg/g), K_L is the Langmuir constant related to the binding energy (L/mg), C_e is the concentration of fluoride in the aqueous solution at equilibrium (mg/L), K_F is the distribution coefficient (L/g), and n is the Freundlich constant. Values of K_L , Q_m , K_F , and n can be determined by fitting the Langmuir and Freundlich models to the observed data.

The kinetic data can be analyzed using the following pseudo first-order and pseudo second-order models [18,19]:

$$q_t = q_e [1 - \exp(-k_1 t)] \quad (3)$$

$$q_t = \frac{k_2 q_e^2 t}{1 + k_2 q_e t} \quad (4)$$

where q_t is the amount of fluoride removed at time t (mg/g), k_1 is the pseudo first-order rate constant (1/h), and k_2 is the pseudo second-order velocity constant (g/mg/h).

The thermodynamic data can be analyzed using the following equations [17]:

$$\log\left(\frac{aq_e}{C_e}\right) = \frac{\Delta S^0}{2.303R} + \frac{-\Delta H^0}{2.303RT} \quad (5)$$

$$\Delta G^0 = \Delta H^0 - T\Delta S^0 \quad (6)$$

where a is the adsorbent dose (g/L), ΔS^0 is the change in entropy, R is the gas constant (= 8.314 J/mol/K), ΔH^0 is the change in enthalpy, T is the absolute tem-

perature, and ΔG^0 is the change in Gibb's free energy. Values of ΔS^0 and ΔH^0 can be determined by plotting $\log(aq_e/C_e)$ versus $1/T$ using Eq. (5), and then value of ΔG^0 can be quantified from Eq. (6).

3. Results and discussion

3.1. Fluoride removal by pyrophyllite

The images of pyrophyllite used in the experiments are presented in Fig. 1. The digital image (Fig. 1a) showed that pyrophyllite particles are white. The FESEM images (Fig. 1b and 1c) indicated that the surface appeared to be rough and heterogeneous in surface topography. The EDS patterns (Fig. 1d) demonstrated that silicon (Si) was evident at the peak position of 1.74 keV as K alpha X-ray signal. Aluminum (Al) was also detected at the peak position of 1.48 keV as K alpha X-ray signal. The chemical composition from XRF analysis (Table 1) showed that the major constituents of pyrophyllite were Si (74.03%) and Al (21.20%). In the FT-IR spectra (Fig. 2), a band recorded at $3,652 \text{ cm}^{-1}$ corresponded to O–H stretching vibrations for OH groups bonded to Al ions. A band at 938 cm^{-1} was attributed to OH bending vibrations for Al–OH groups. Note that other properties (BET surface area, XRD pattern) related to pyrophyllite are described in the later section.

The equilibrium isotherms of fluoride on pyrophyllite with different particle sizes are presented in Fig. 3. The equilibrium isotherm constants are summarized in Table 2. In the Freundlich model, the distribution coefficient (K_F) was in the range from 0.174 to 0.247 L/g, while the Freundlich constant (n) was between 0.224 and 0.250. In the Langmuir model, the Langmuir constant (K_L) was in the range from 0.246 to 0.310 L/mg, while the removal capacity (Q_m) was between 0.488 and 0.649 mg/g. The correlation coefficient (R^2) of the Freundlich model was greater than that of the Langmuir model, indicating that the Freundlich isotherm was appropriate at describing the experimental result. Among the particles tested, the one with particle size of <0.15 mm showed the highest adsorption capacity of 0.737 mg/g, which was in the ranges of the removal capacity for clays/modified clays (0.045–4.24 mg/g) reported in the literature (Table 3).

The sorption kinetics of fluoride in pyrophyllite (size <0.15 mm; initial fluoride concentration = 10 mg/L) is shown in Fig. 4. The sorption reached equilibrium around 24 h of reaction time. Model parameters for the pseudo first-order and pseudo second-order models obtained from the kinetic experiments are provided in

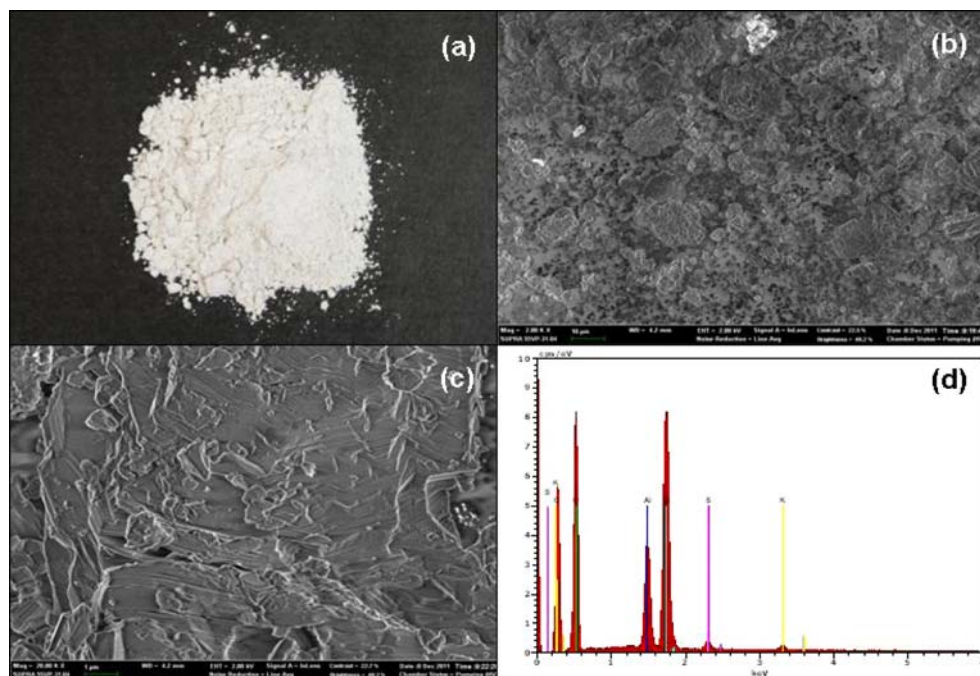


Fig. 1. Pyrophyllite used in the experiment: (a) digital image; (b) field emission scanning electron micrograph (FESEM, bar = 10 μm); (c) FESEM (bar = 1 μm); (d) X-ray spectrum (EDS).

Table 1

Chemical composition of pyrophyllite used in the experiment (wt.%, from XRF data)

SiO ₂	Al ₂ O ₃	SO ₃	Fe ₂ O ₃	TiO ₂	K ₂ O	Cr ₂ O ₃	SrO	CaO	CuO	ZrO ₂	Total
74.03	21.20	2.38	1.885	0.152	0.084	0.081	0.073	0.072	0.023	0.020	100

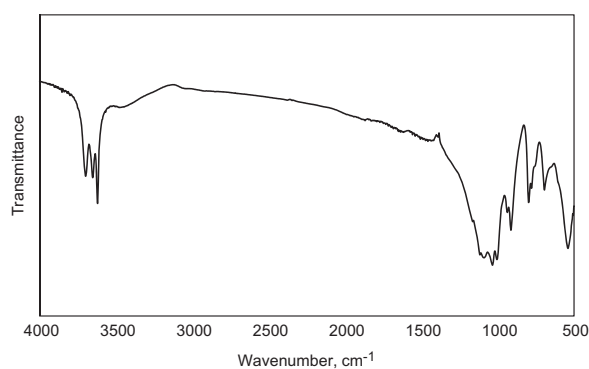


Fig. 2. FT-IR spectra of pyrophyllite used in the experiments.

Table 4. In the pseudo first-order model, the value of q_e was 0.263 mg/g while the value of k_1 was 0.244 1/h. The value of q_e from the pseudo second-order model was greater than that from the pseudo first-order

model. The value of q_e was 0.297 mg/g, while the values of k_2 was 1.023 g/mg h. The correlation coefficients (R^2) indicated that the pseudo first-order model described the kinetic data better than the pseudo second-order model. The adsorption of fluoride ions (F^-) to pyrophyllite surfaces could be described by ligand exchange mechanism. In the adsorption process, fluoride ions could replace hydroxyl ions (OH^-) on the surfaces of pyrophyllite ($\text{Al-OH} \rightarrow \text{Al-F}$). Additionally, below pH_{pzc} where pyrophyllite is positively charged, electrostatic attraction could occur between negatively-charged fluoride ions and positively-charged surfaces of pyrophyllite ($\text{Al-OH}_2^+ \leftrightarrow \text{F}^-$) [22]. Note that the pH_{pzc} of pyrophyllite was determined to be 9.2.

The thermodynamic data and analysis for fluoride sorption to pyrophyllite is presented in Fig. 5. Thermodynamic parameters are provided in Table 5. As shown in Fig. 5a, fluoride adsorption to pyrophyllite increased with increasing temperature from 25 to 45 $^\circ\text{C}$, demonstrating that the sorption process was

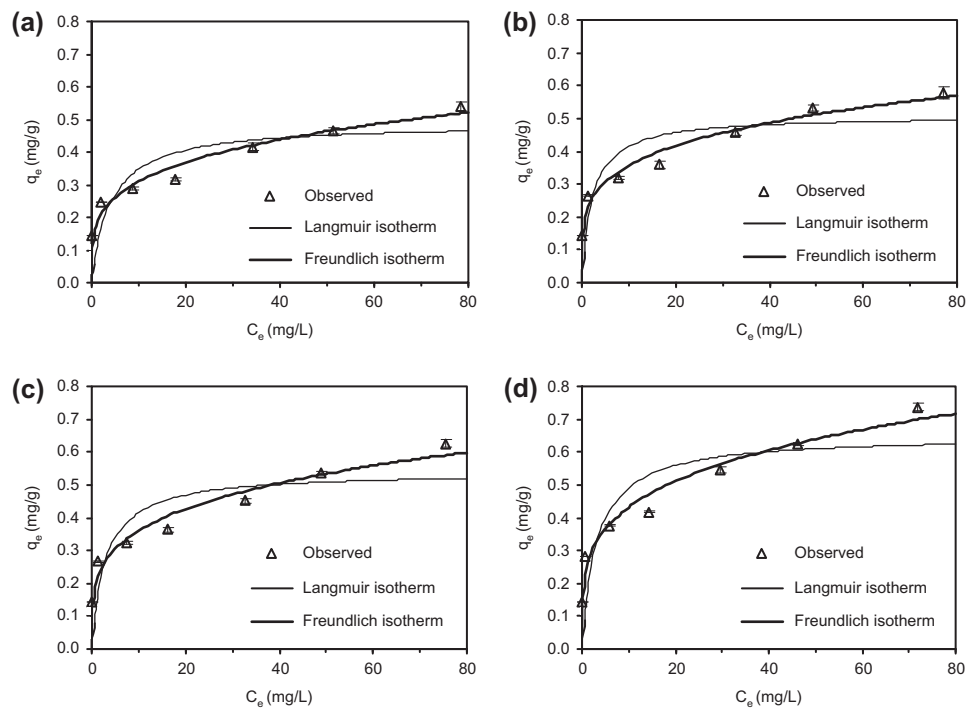


Fig. 3. Equilibrium batch data and model fit for fluoride adsorption to pyrophyllite with different particle sizes (mm): (a) 0.42–0.85; (b) 0.25–0.42; (c) 0.15–0.25; (d) <0.15. Equilibrium isotherm constants are provided in Table 2.

Table 2
Equilibrium isotherm constants for fluoride adsorption by pyrophyllite with different particle sizes

Particle size (mm)	Freundlich isotherm model			Langmuir isotherm model		
	K_F (L/g)	n	R^2	K_L (L/mg)	Q_m (mg/g)	R^2
0.42–0.85	0.174	0.250	0.942	0.246	0.488	0.653
0.25–0.42	0.213	0.224	0.943	0.440	0.508	0.646
0.15–0.25	0.204	0.246	0.928	0.333	0.539	0.640
<0.15	0.247	0.244	0.948	0.310	0.649	0.701

endothermic (Fig. 5a). The positive value of ΔH^0 also indicated the endothermic nature of fluoride sorption. The positive value of ΔS^0 showed that the randomness increased at the interface between solid and solution during the sorption process. The negative value of ΔG^0 indicated that the sorption process was spontaneous. This result confirms well with the reports of other researchers who examined the endothermic nature of fluoride adsorption to clay particles such as Mg/Al/Fe layer double hydroxides [23], magnesium incorporated bentonite [10], attapulgite [24], and micronized kaolinite [25]. However, Goswami and Purkait [17] who examined the effect of temperatures on fluoride sorption to pyrophyllite reported that the

sorption was exothermic, decreasing with increasing temperature from 24 to 60 °C.

3.2. Effects of adsorbent dose, pH and anions

The effect of pyrophyllite dose on fluoride sorption in pyrophyllite (particle size <0.15 mm; initial fluoride concentration = 10 mg/L) is presented in Fig. 6. The removal percent increased from 25.0 to 98.5% with increasing pyrophyllite doses from 0.05 to 2.0 g/L. Meanwhile, adsorption capacity decreased from 1.414 to 0.139 mg/g with increasing pyrophyllite doses. Results indicated that initial fluoride concentration of

Table 3
Fluoride sorption capacities of clays reported in the literature

Adsorbent	Sorption capacity (mg/g)	Fluoride concentration range (mg/L)	Ref.
China clay	0.66	10.0	[4]
Montmorillonite	1.485	3.0	[5]
Algerian clay	1.013	1.0–6.0	[7]
Acid activated kaolinite	0.0045	3.0	[8]
Chemically modified bentonite	4.24	-	[9]
Magnesium incorporated bentonite	2.26	5.0	[10]
Pyrophyllite	2.2	2.0–12.0	[17]
Kaolinite	0.667	5.0	[20]
Montmorillonite	0.263	2.0–120.0	[21]

10 mg/L could be reduced to <1.5 mg/L at pyrophyllite dose ≥ 1.0 g/L.

The effect of solution pH on fluoride removal in pyrophyllite (particle size <0.15 mm; initial fluoride concentration = 10 mg/L) is shown in Fig. 7. The adsorption capacity was relatively constant when pH increased from 4.0 to 5.9, leading to values of 0.278 and 0.276, respectively. As the solution pH further increased and approached 9.0, the adsorption capacity decreased slightly to 0.260 mg/g, indicating that fluoride removal in pyrophyllite was not sensitive to solution pH changes between 4.0 and 9.0 under given experimental conditions. However, the adsorption capacity decreased considerably to 0.146 mg/g at pH 2.9. In highly acidic pH, fluoride could exist preferably as the form of HF, and so the adsorption of fluoride to pyrophyllite could be reduced greatly. At pH 11.0, the adsorption capacity decreased sharply to 0.004 mg/g. In highly alkaline pH, fluoride could exist preferably as NaF form due to addition of NaOH into solution, which results in the sharp decrease of fluoride adsorption to pyrophyllite. Our results conform well with the report of Goswami and Purkait [17]

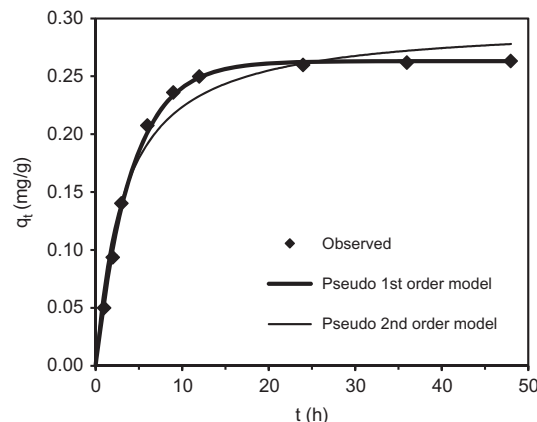


Fig. 4. Kinetic batch data and model fit for fluoride adsorption to pyrophyllite (particle size <0.15 mm; initial fluoride concentration = 10 mg/L). Kinetic model parameters are provided in Table 4.

who investigated the adsorption of fluoride to pyrophyllite (initial fluoride concentration = 10 mg/L). They reported that more than 80% fluoride was adsorbed between pH 4.9 and pH 10.0, whereas the fluoride adsorption decreased in highly acidic pH (pH < 4.0) and highly alkaline pH (pH > 10.0).

The effect of anions on the removal of fluoride in pyrophyllite (particle size <0.15 mm; initial fluoride concentration = 10 mg/L) is presented in Fig. 8. Chloride (Cl⁻) and nitrate (NO₃⁻), monovalent anions, showed minimal effect on the removal of fluoride in pyrophyllite at concentrations ranging from 0.5 to 1 mM. This result agreed well with the previous reports [5,25], showing that the effects of Cl⁻ and NO₃⁻ on fluoride removal in clay adsorbents was negligible. Meanwhile, divalent anions such as sulfate (SO₄²⁻), phosphate (HPO₄²⁻), and carbonate (CO₃²⁻) profoundly interfered with the removal of fluoride in pyrophyllite. Goswami and Purkait [17] reported that the adsorption of fluoride to pyrophyllite decreased slightly from 84 to 79% with increasing sulfate ions from 3.1 to 12.5 mg/L. Divalent anions are known to have a higher affinity to adsorbents than monovalent anions. Our results indicated that the removal of fluoride in pyrophyllite was most affected by CO₃²⁻. At the given experimental conditions, the impact of

Table 4
Kinetic model parameters obtained from model fitting to experimental data

Pseudo first-order model			Pseudo second-order model		
q_e (mg/g)	k_1 (1/h)	R^2	q_e (mg/g)	k_2 (g/mg h)	R^2
0.263	0.244	0.998	0.297	1.023	0.978

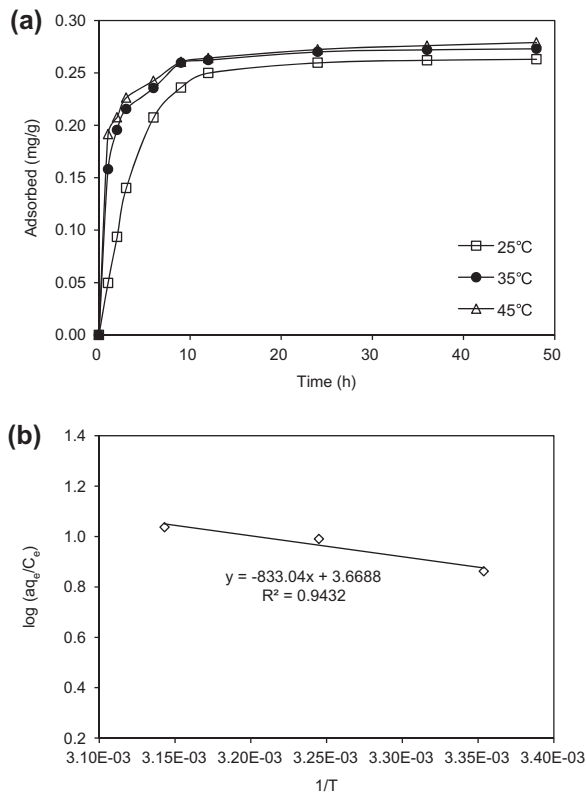


Fig. 5. Thermodynamic data and analysis for fluoride adsorption to pyrophyllite (particle size <0.15 mm; initial fluoride concentration = 10 mg/L): (a) effect of temperature on fluoride sorption; (b) determination of thermodynamic parameter. Thermodynamic parameters are provided in Table 5.

Table 5
Thermodynamic parameters for fluoride adsorption to pyrophyllite

Temperature (°C)	ΔH° (kJ/mol)	ΔS° (J/K mol)	ΔG° (kJ/mol)
25	15.95	70.25	-4.99
35			-5.70
45			-6.40

the divalent anions was in the order of $SO_4^{2-} < HPO_4^{2-} < CO_3^{2-}$.

3.3. Effect of thermal treatment of pyrophyllite

The adsorption capacities for fluoride removal by pyrophyllite thermally treated under different temperatures are provided in Fig. 9. Thermal treatment influenced the adsorption capacity of pyrophyllite. In given experimental conditions (adsorbent

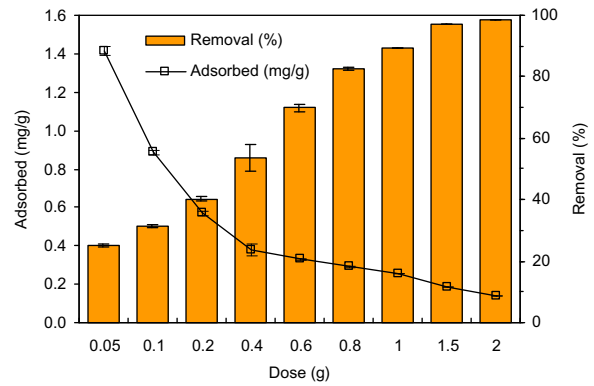


Fig. 6. Effect of pyrophyllite dose on fluoride adsorption (particle size <0.15 mm; initial fluoride concentration = 10 mg/L).

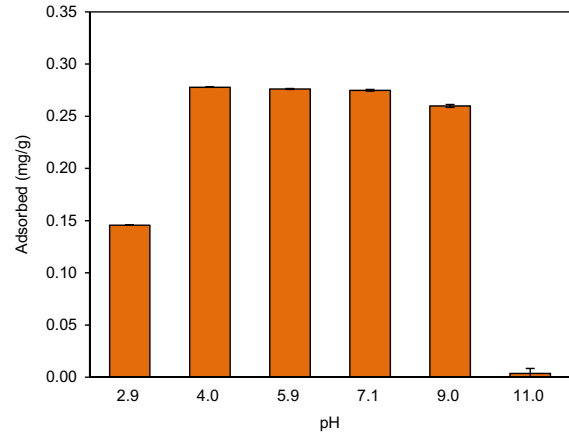


Fig. 7. Effect of solution pH on fluoride adsorption to pyrophyllite (particle size <0.15 mm; initial fluoride concentration = 10 mg/L).

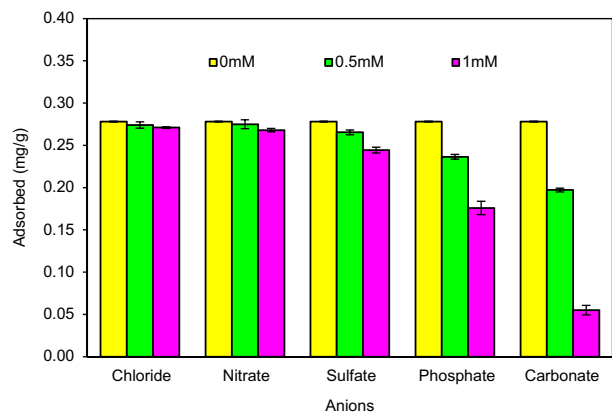


Fig. 8. Effect of anions on fluoride adsorption to pyrophyllite (particle size <0.15 mm; initial fluoride concentration = 10 mg/L).

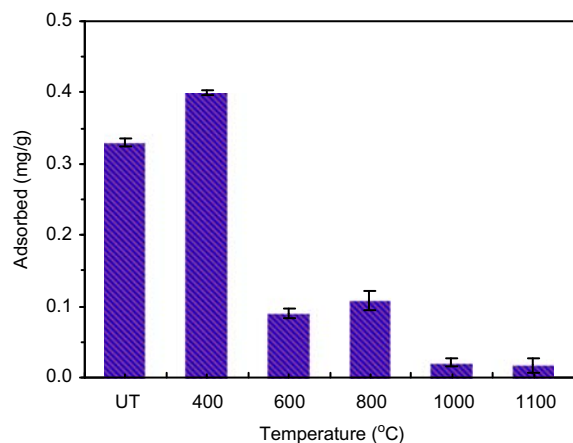


Fig. 9. Effect of thermal treatment of pyrophyllite on fluoride adsorption (UT=untreated; particle size < 0.15 mm; initial fluoride concentration = 10 mg/L).

dosage = 0.6 g; fluoride concentration = 10 mg/L; solution volume = 30 mL), the adsorption capacity (= 0.399 mg/g) was the highest in the adsorbent treated at 400 °C (A-400), which is 21% higher than that (= 0.329 mg/g) of untreated pyrophyllite (UT). At higher temperatures (600, 800 °C), the adsorption capacities of A-600 and A-800 sharply decreased

to ~0.10 mg/g. At 1,000 and 1,100 °C, the adsorption capacities of A-1000 and A-1100 decreased further to ~0.02 mg/g.

This result could be attributed to the fact that thermal treatment could alter the mineralogical and physical properties of pyrophyllite. XRD patterns of pyrophyllite treated under different temperatures are presented in Fig. 10. Also, the mineralogical property and BET surface area of thermally treated pyrophyllite are provided in Table 6. Untreated pyrophyllite (UT) showed the general XRD pattern found in the literature [11], possessing the peaks of quartz (SiO_2 , hexagonal), dickite ($\text{Al}_2\text{Si}_2\text{O}_5(\text{OH})_4$), and pyrophyllite ($\text{Al}_2\text{Si}_4\text{O}_{10}(\text{OH})_2$). A-400 had the same XRD pattern as UT with the peaks of quartz, dickite, and pyrophyllite. In addition, A-400 had the surface area of $1.673 \text{ m}^2/\text{g}$, which is about 24% higher than that (= $1.342 \text{ m}^2/\text{g}$) of UT. Above 600 °C, however, the general XRD pattern of pyrophyllite was disappeared. A-600 and A-800 had the peaks of quartz with the surface areas of 1.935 and $1.475 \text{ m}^2/\text{g}$, respectively. At 1,000 and 1,100 °C, the peaks of mulite ($\text{Al}_6\text{Si}_2\text{O}_{13}$) and cristobalite (SiO_2 , tetragonal) were appeared along with the quartz peaks. A-1000 and A-1100 had the surface areas of 0.992 and $0.420 \text{ m}^2/\text{g}$, respectively.

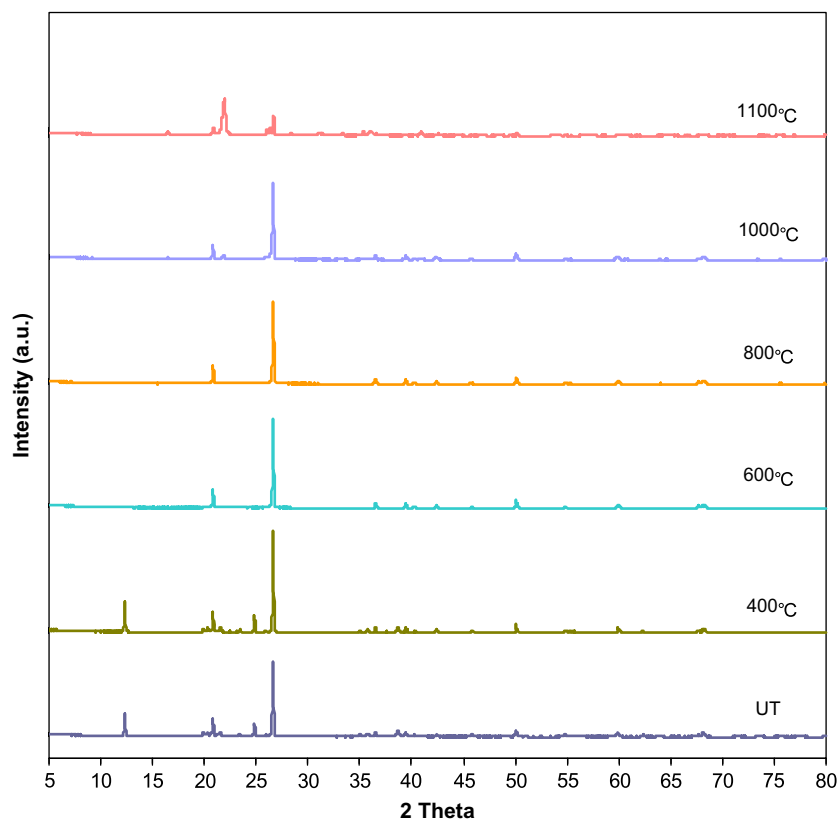


Fig. 10. X-ray diffraction patterns of pyrophyllite thermally treated at different temperatures (UT = untreated).

Table 6
Characteristics of pyrophyllite thermally treated at different temperatures

Temperature (°C)	UT	400	600	800	1,000	1,100
BET surface area (m ² /g)	1.342	1.673	1.935	1.475	0.992	0.420
Properties (XRD peak)	Q, D, Py	Q, D, Py	Q	Q	Q, C, M	Q, C, M

Note: UT: untreated; Q: quartz; D: dickite; Py: pyrophyllite; C: cristobalite; M: mulite.

4. Conclusions

In this study, the removal of fluoride by pyrophyllite was examined. Results showed that pyrophyllite was effective in the removal of fluoride (maximum sorption capacity = 0.737 mg/g). Kinetic test indicated that fluoride sorption to pyrophyllite arrived at equilibrium around 24 h. Thermodynamic test indicated that fluoride sorption to pyrophyllite was endothermic. Results also demonstrated that fluoride removal was not sensitive to solution pH between 4.0 and 9.0. The influence of divalent anions (SO₄²⁻, CO₃²⁻, HPO₄²⁻) on the fluoride removal was important. In addition, pyrophyllite thermally treated at 400°C had the higher sorption capacity than that of untreated pyrophyllite. This study demonstrates the potential use of pyrophyllite for fluoride removal from water.

Acknowledgment

This research was supported by the National Research Foundation of Korea, funded by the Ministry of Education, Science and Technology, Republic of Korea (grant number 2011-0009688).

References

- [1] S. Ayoob, A.K. Gupta, Fluoride in drinking water: A review on the status and stress effects, *Crit. Rev. Environ. Sci. Technol.* 36 (2006) 433–487.
- [2] A. Bhatnagar, E. Kumar, M. Sillanpää, Fluoride removal from water by adsorption: A review, *Chem. Eng. J.* 171 (2011) 811–840.
- [3] M. Mohapatra, S. Anand, B.K. Mishra, D.E. Giles, P. Singh, Review of fluoride removal from drinking water, *J. Environ. Manage.* 91 (2009) 67–77.
- [4] A.K. Chaturvedi, K.C. Pathak, V.N. Singh, Fluoride removal from water by adsorption on china clay, *Appl. Clay Sci.* 3 (1988) 337–346.
- [5] G. Karthikeyan, A. Pius, G. Alagumuthu, Fluoride adsorption studies of montmorillonite clay, *Indian J. Chem. Technol.* 12 (2005) 263–272.
- [6] L. Lv, Defluoridation of drinking water by calcined MgAl- CO_3 layered double hydroxides, *Desalination*. 208 (2007) 125–133.
- [7] A. Ramdani, S. Taleb, A. Benghalem, N. Ghaffour, Removal of excess fluoride ions from Saharan brackish water by adsorption on natural materials, *Desalination*. 250 (2010) 408–413.
- [8] P.K. Gogoi, R. Baruah, Fluoride removal from water by adsorption on acid activated kaolinite clay, *Indian J. Chem. Technol.* 15 (2008) 500–503.
- [9] S.P. Kamble, P. Dixit, S.S. Rayalu, N.K. Labhsetwar, Defluoridation of drinking water using chemically modified bentonite clay, *Desalination*. 249 (2009) 687–693.
- [10] D. Thakre, S. Rayalu, R. Kawade, S. Meshram, J. Subrt, N. Labhsetwar, Magnesium incorporated bentonite clay for defluoridation of drinking water, *J. Hazard. Mater.* 180 (2010) 122–130.
- [11] A. Bentayeb, M. Amouric, J. Olives, A. Dekayir, A. Nadiri, XRD and HRTEM characterization of pyrophyllite from Morocco and its possible applications, *Appl. Clay Sci.* 22 (2003) 211–221.
- [12] R. Keren, D.L. Sparks, Effect of pH and ionic strength on boron adsorption by pyrophyllite, *Soil Sci. Soc. Am. J.* 58 (1994) 1095–1100.
- [13] S. Saxena, M. Prasad, S.S. Amritphale, N. Chandra, Adsorption of cyanide from aqueous solutions at pyrophyllite surface, *Sep. Purif. Technol.* 24 (2001) 263–270.
- [14] A. Gücek, S. Şener, S. Bilgen, M.A. Mazmanlı, Adsorption and kinetic studies of cationic and anionic dyes on pyrophyllite from aqueous solutions, *J. Colloid Interf. Sci.* 286 (2005) 53–60.
- [15] M. Prasad, S. Saxena, Attenuation of divalent toxic metal ions using natural sericitic pyrophyllite, *J. Environ. Manage.* 88 (2008) 1273–1279.
- [16] N. Gupta, M. Prasad, N. Singhal, V. Kumar, Modeling the adsorption kinetics of divalent metal ions onto pyrophyllite using the integral method, *Ind. Eng. Chem. Res.* 48 (2009) 2125–2128.
- [17] A. Goswami, M.K. Purkait, Kinetic and equilibrium study for the fluoride adsorption using pyrophyllite, *Sep. Sci. Technol.* 46 (2011) 1797–1807.
- [18] Y.S. Ho, G. McKay, Pseudo-second order model for sorption processes, *Process Biochem.* 34 (1999) 451–465.
- [19] T. Mathialagan, T. Viraraghavan, Adsorption of cadmium from aqueous solutions by vermiculite, *Sep. Sci. Technol.* 38 (2003) 57–76.
- [20] M. Srimurali, A. Pragathi, J. Karthikeyan, A study on removal of fluorides from drinking water by adsorption onto low-cost materials, *Environ. Pollut.* 99 (1998) 285–289.
- [21] A. Tor, Removal of fluoride from an aqueous solution by using montmorillonite, *Desalination*. 201 (2006) 267–276.
- [22] S. Ayoob, A.K. Gupta, V.T. Bhat, A conceptual overview on sustainable technologies for the defluoridation of drinking water, *Crit. Rev. Environ. Sci. Technol.* 38 (2008) 401–470.
- [23] W. Ma, N. Zhao, G. Yang, L. Tian, R. Wang, Removal of fluoride ions from aqueous solution by the calcination product of Mg–Al–Fe hydrotalcite-like compound, *Desalination*. 268 (2011) 20–26.
- [24] J. Zhang, S. Xie, Y.S. Ho, Removal of fluoride ions from aqueous solution using modified attapulgite as adsorbent, *J. Hazard. Mater.* 165 (2009) 218–222.
- [25] S. Meenakshi, C.S. Sundaram, R. Sukumar, Enhanced fluoride sorption by mechanochemically activated kaolinites, *J. Hazard. Mater.* 153 (2008) 164–172.